Explanation of the simplicity of the quadrupole moments recently observed in Cd isotopes from covariant density functional theory

P. W. Zhao (赵鹏巍),[1] S. Q. Zhang (张双全),[1] and J. Meng (孟杰)[1,2,3]

[1]*State Key Laboratory of Nuclear Physics and Technology, School of Physics, Peking University, Beijing 100871, China*
[2]*School of Physics and Nuclear Energy Engineering, Beihang University, Beijing 100191, China*
[3]*Department of Physics, University of Stellenbosch, Stellenbosch, South Africa*

The simplicity in the nuclear quadrupole moments reported recently in $^{107-129}$Cd, i.e., a linear increase of the $11/2^-$ quadrupole moments, is investigated microscopically with the covariant density functional theory. Using the newly developed functional PC-PK1, the quadrupole moments as well as their linear increase tendency with the neutron number are excellently reproduced without any *ad hoc* parameters. The core polarization is found to be very important and contributes almost half of the quadrupole moments. The simplicity of the linear increase is revealed to be due to the pairing correlation which smears out the abrupt changes induced by the single-particle shell structure.

The electric and magnetic moments are fundamental observables in understanding matter structure ranging from physics to chemistry. In nuclear physics, thanks to the simple and well-known structure of the electromagnetic interaction, the study of electric and magnetic moments and transition probabilities provides unique opportunity for detailed understanding of nuclear structure and has attracted the attention of nuclear physicists since the early days [1].

The electric quadrupole moment is the most important multipole expansion of a nuclear electric moment, reflecting the extent to which the nuclear charge distribution deviates from sphericity and representing the most important collective excitations of the nucleus. In fact, the electric quadrupole moment in deuteron [2] provides the first evidence for the need of a tensor term in the nuclear interaction [3], which turns out to be essential in understanding the variation of the nuclear shell structure [4]. Many hot topics in nuclear physics including exotic deformation [5], shape coexistence [6], and shell evolution [7] are rooted in the study of the nuclear electric quadrupole moment.

In a recent paper [8], the quadrupole moments of neutron-rich isotopes of cadmium up to the $N = 82$ shell closure were investigated by high-resolution laser spectroscopy, and a linear increase of the $11/2^-$ quadrupole moments was found to act well even beyond the $h_{11/2}$ shell. A similar phenomenon has also been discussed for the $i_{13/2}$ isomers of lead and mercury isotopes previously [9]. However, it is the first in Ref. [8] to demonstrate that the linear behavior can persist even beyond a single shell, and the high experimental precision achieved provides a rigorous calibration for theories. As mentioned in Ref. [10], the result reported by Yordanov *et al*. [8] is a success for the shell model and the concept of pairing of neutrons and of protons to produce a simple and persistent structure in a long isotopic chain. The challenge to the theorists now is to explain this simplicity in a microscopic level.

The extreme single-particle shell model, which has played a major role in clarifying nuclear structure [11], is widely used to describe nuclear quadrupole moments. In this model, the quadrupole moment of an odd-proton (neutron) nucleus with spin I is determined by the unpaired proton (neutron) in the orbital with the total angular momentum $j = I$. For a nucleus with one particle or hole around the doubly magic nucleus, e.g., ^{208}Pb [12], a good agreement with the experimental quadrupole moments can be achieved with the introduction of the effective charges. In such a way, the interaction between the valence nucleons and the core nucleons or the core polarization can be effectively taken into account.

For a nucleus with n valence particles (holes) in an orbital j coupled to a total spin I, the shell model predicts that the quadrupole moments of nuclear states described by such a pure configuration would follow a simple linear relation with respect to the number of valence protons [11] or neutrons [13]. In general, the corresponding formalism can be given in the seniority scheme as [14]

$$\langle j^n | \hat{Q} | j^n \rangle = \frac{2j + 1 - 2n}{2j + 1 - 2\nu} \langle j^\nu | \hat{Q} | j^\nu \rangle, \tag{1}$$

with ν being the number of the unpaired valence nucleons. Due to this very characteristic linear behavior with respect to the number of valence nucleons, the electric quadrupole moment is believed to provide a stringent test of the model.

Density functional theory (DFT) plays a very important role in describing the many-body problems in a microscopic way. It has achieved great success in all quantum mechanical many-body systems, e.g., in Coulombic systems. In nuclear physics, with spin and isospin degrees of freedom, the situation is much more complicated due to the strong nucleon-nucleon forces. Because Lorentz invariance is one of the underlying symmetries for the quantum chromodynamics of the strong interaction, the covariant density functionals [15–18] are of particular interest in nuclear physics. This symmetry not only provides us a consistent treatment of the spin degrees of freedom, but also puts stringent restrictions on the number of parameters in the corresponding functionals without reducing the quality of the agreement with experimental data [19].

In this Rapid Communication, the quadrupole moments of the Cd isotopes together with their linear simplicity shown in the most up-to-date data will be investigated in the framework

of covariant DFT (CDFT) in a self-consistent and microscopic way. The major advantages of the present framework include (1) the core polarization effects are fully taken into account and there is no need to introduce a factitious effective charge, (2) the pairing correlation is treated self-consistently by the corresponding pairing functional, (3) the density functional is universal for all nuclei throughout the periodic chart, and the present investigation is expected to be reliable and to have predictive power, and (4) a microscopic picture of the nuclear quadrupole moments can be provided in terms of intrinsic shapes and single-particle shells self-consistently.

Covariant density functional theory starts from an effective Lagrangian, and the corresponding Kohn-Sham equations have the form of a Dirac equation:

$$[\boldsymbol{\alpha} \cdot \boldsymbol{p} + \beta(m + S) + V]\psi_k = \epsilon_k \psi_k, \tag{2}$$

with effective potentials $S(\boldsymbol{r})$ and $V(\boldsymbol{r})$ derived from this Lagrangian, which are connected in a self-consistent way to the densities; for details, see Refs. [15–18]. The iterative solution of this equation yields the single-particle energies and wave functions, binding energies, quadrupole moments, etc. It should be noted that the calculations here are carried out in the intrinsic frame, and the measured quadrupole moment Q for an axially symmetric nucleus is related to the intrinsic quadrupole moment Q_0 through the relation

$$Q = \frac{3K^2 - I(I+1)}{(I+1)(2I+3)} Q_0, \tag{3}$$

where K is the projection of the total spin I onto the symmetry axis of the deformed nucleus. Note that the moment in Eq. (3) includes only the collective part associated with the average deformation of the intrinsic state [1]. Further investigation should go beyond the mean field level such as including the configuration mixing and is beyond the scope of the present work.

The Dirac equation (2) is solved on the basis of an axially symmetric harmonic oscillator potential [20] with 14 major shells. The point-coupling functional PC-PK1 [21] is used for the Lagrangian without any additional parameters, and the pairing correlations are taken into account by the Bardeen-Cooper-Schrieffer (BCS) method with a zero-range δ force. The pairing strength in Ref. [21] is adopted, which is adjusted together with PC-PK1 in a smooth cutoff pairing window. By carrying out calculations with the triaxial degree of freedom, it is found that the triaxiality for the present Cd isotopes is negligible. Therefore, the effective potentials S and V are considered to be axially deformed.

Since we are focusing on the $11/2^-$ quadrupole moments of the odd-A Cd isotopes observed in Ref. [8], the last unpaired neutron will block its occupied level in the BCS calculations, i.e., the Pauli principle prevents this level from the scattering process of nucleon pairs by the pairing correlations. In practical calculations, the single-particle orbital $h_{11/2}$ with the third projection of the total angular momentum $j_z = 11/2$ is always blocked in order to obtain the nuclear states with $K = 11/2$. Meanwhile, the time-odd fields are neglected in the calculations since they have little influence on the quadrupole moments.

Concretely, we adopt the standard blocking method [22], where the ground state of an odd system is described by the wave function

$$a_{k_1}^{\dagger}|\text{BCS}\rangle = a_{k_1}^{\dagger} \prod_{k \neq k_1}(u_k + v_k a_k^{\dagger}|a_{-k}^{\dagger}|0\rangle). \tag{4}$$

Here, $|0\rangle$ denotes the vacuum state, and k_1 the blocked single-particle orbit (here the orbit $j_z^{\pi} = 11/2^-$). This orbit has to be excluded in the calculation of pairing energy. Meanwhile, the Fermi energy λ is determined by $N = 1 + 2\sum_{k \neq k1 > 0} v_k^2$ with N being the neutron number and v_k^2 being the occupation probability of the single-particle orbit k.

In the upper panel of Fig. 1, the calculated quadrupole moments in CDFT with and without pairing correlation are shown in comparison with the data [8]. One can see that when the
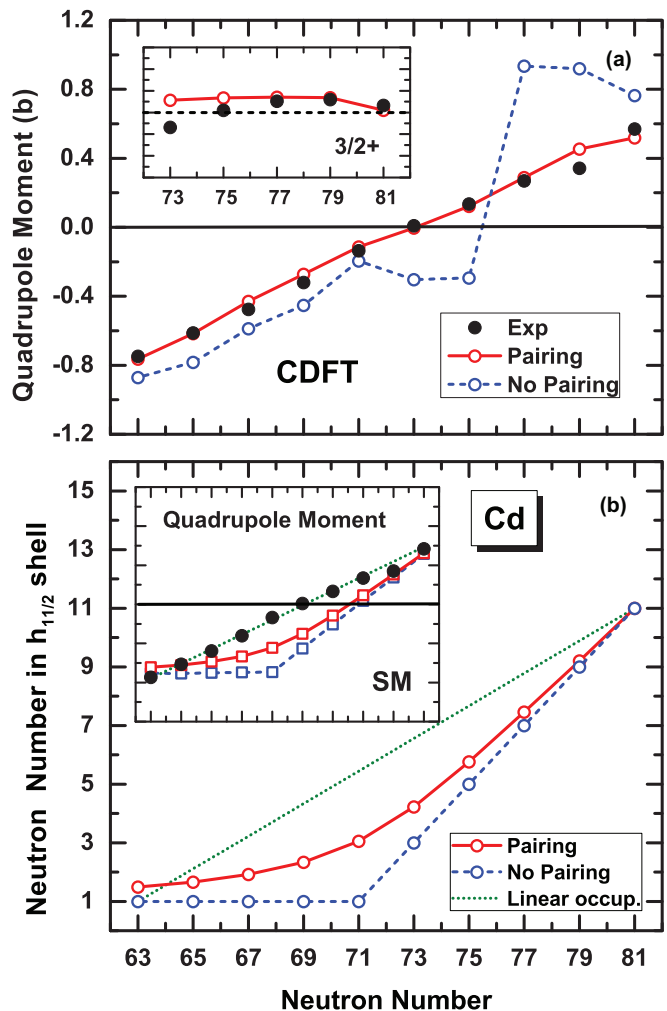

FIG. 1. (Color online) Calculated quadrupole moments (a) and the occupation neutrons in the $h_{11/2}$ shell (b) in the CDFT with (full lines) and without (dashed lines) the pairing correlation for Cd isotopes. The data (solid dots) are taken from Ref. [8]. The dotted line in (b) represents a linear occupation assumption proposed in [8]. Inset (a): Calculated quadrupole moments in CDFT with a pairing correlation for the $3/2^+$ states in comparison with the data [8]. Inset (b): Comparison between the observed quadrupole moments [8] and the calculated ones with Eq. (1), in which the number of neutrons n is either the CDFT results with (full line) or without (dashed line) the pairing correlation or from the linear occupation assumption [8].

pairing correlations are taken into account, the experimental quadrupole moments together with the corresponding linear increase tendency are excellently reproduced in a microscopic and self-consistent way. Without pairing, however, one can clearly find two distinct features: for nuclei with $N \leqslant 71$, the calculated quadrupole moments are slightly smaller than the observed ones but still hold the linear increase tendency; for nuclei with $N \geqslant 71$, the calculated results deviate not only from the data but also from the linear tendency. This indicates that the mechanism for the linear increase of the quadrupole moments may be different for nuclei with their neutron number smaller and larger than 71.

In the lower panel of Fig. 1, similar features can also be seen for the neutron occupation number in the $h_{11/2}$ shell. Without pairing, there is always one neutron sitting in the $h_{11/2}$ shell for nuclei with $N \leqslant 71$, and this number starts to increase linearly from one for ^{119}Cd to 11 for ^{129}Cd. As a result, in the case without pairing, the increase of the neutrons in the $h_{11/2}$ shell shows a clear inflexion point at the nucleus ^{119}Cd, which is consistent with the varying features of the quadrupole moments as shown in Fig. 1(a). Such an abrupt inflexion point can be smoothed admirably by the pairing effects. Obviously,

the neutron occupation number in the $h_{11/2}$ shell with the pairing correlation does not follow the linear occupation assumption [dotted line in Fig. 1(b)] proposed in Ref. [8].

In the inset of Fig. 1(b), adopting the linear occupation assumption, the experimental quadrupole moments together with the corresponding linear increase tendency can also be reproduced by Eq. (1). In the calculation, the single-particle quadrupole moment $\langle j^v | \hat{Q} | j^v \rangle|_{v=1}$ of the $h_{11/2}$ shell in Eq. (1) is estimated by $-e_f \langle r^2 \rangle (2j-1)/(2j+2)$ with the effective charge $e_f = 2.5e$ and $\langle r^2 \rangle$ being calculated in CDFT, and it is found to be nearly constant for all the Cd isotopes. This explanation, however, is based on the linear occupation assumption shown as a dotted line in Fig. 1(b). By replacing this fictitious occupation with the microscopic and self-consistent occupation obtained from CDFT, one can easily find that the calculated results fail to reproduce the data, as shown in the inset of Fig. 1(b), no matter whether the pairing correlation is included or not. It should be mentioned that the calculated quadrupole moments here, similarly as in Ref. [8], have been scaled with a small offset term Q_{const} around 150 mb.

In the microscopic CDFT calculation, the quadrupole moment comes from all the protons in a nucleus. To understand
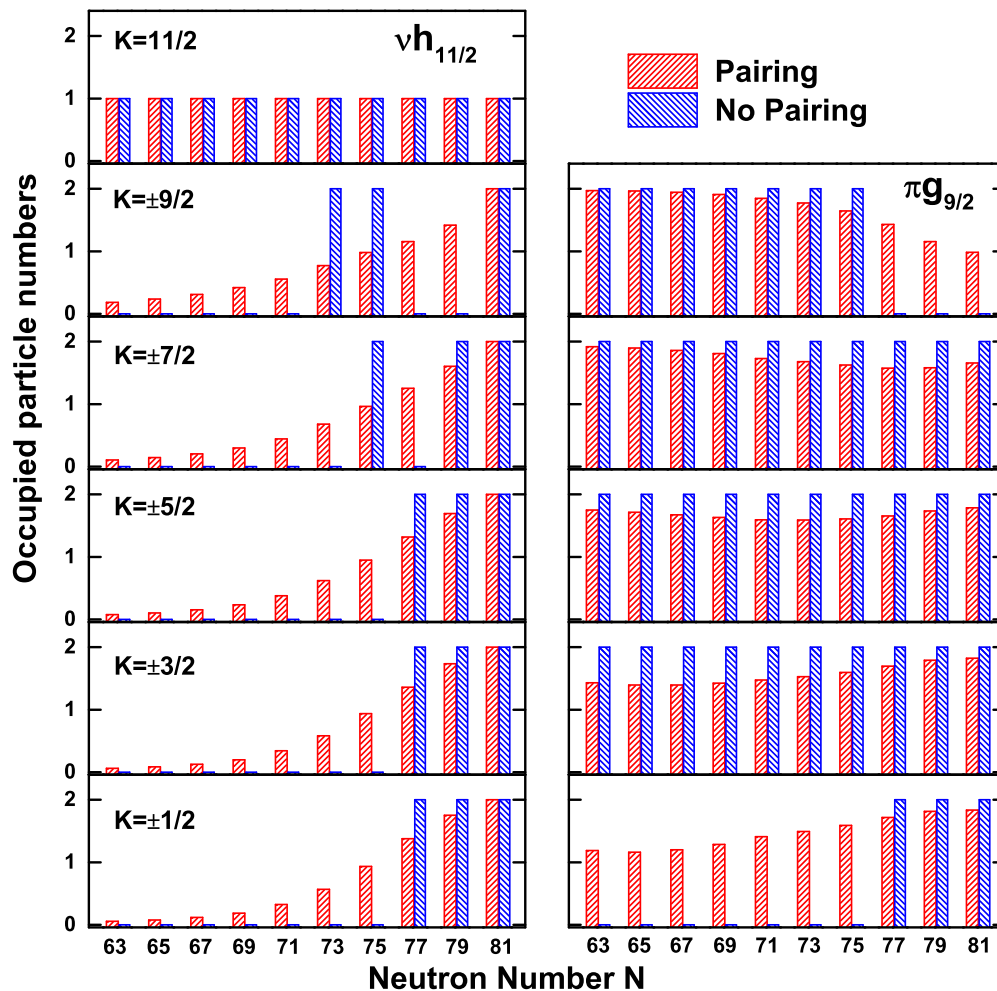

FIG. 2. (Color online) Occupied particle numbers for single-particle orbitals with K, the third component of the angular momentum in the neutron $\nu h_{11/2}$ shell (left panels) and the proton $\pi g_{9/2}$ shell (right panels), obtained from the CDFT calculations with and without pairing correlation.

the microscopic origin for the observed linear behavior of the quadrupole moments, we show in Fig. 2 the occupied particle numbers for single-particle orbitals with K the third component of the angular momentum in the neutron $\nu h_{11/2}$ shell and the proton $\pi g_{9/2}$ shell. Note that the degeneracy of each orbital here is 2, since an orbital with K has the same energy as that with $-K$.

Without pairing correlation, since the neutron orbital $K = 11/2$ is blocked, there is always one neutron in this orbital. The occupation of neutrons in other orbitals can be classified into two distinct cases. For nuclei with $N \leqslant 71$, the increasing neutrons occupy other low j shells instead of the $h_{11/2}$ shell. Due to the occupation of the high $K = 11/2$ orbital, these nuclei have their neutron density distributions of oblate shapes. Moreover, because there is a closure of the positive parity subshell at $N = 70$, the neutron density distributions are driven toward a spherical shape with the increase of the neutron number. Because of the attractive proton and neutron interaction, the proton density distributions evolve in a similar manner as the neutron ones with the increasing neutron number, and thus the quadrupole moments will approach zero smoothly.

For nuclei with $N \geqslant 71$, it shows that the neutrons favor high K orbitals for nuclei with $N \leqslant 75$, while they favor low K orbitals for nuclei with $N \geqslant 77$. This indicates that with the increasing neutron number, the neutron density distribution changes from an oblate shape to a prolate shape near $N = 76$. Similar evolution appears for the protons as well. It leads to an abrupt change of the single-proton level structure, and accordingly an abrupt jump of the quadrupole moments near $N = 76$ as shown in Fig. 1(a).

With the pairing correlation, however, the occupied particle numbers for all orbitals vary smoothly. It shows that the proton occupation of the low K orbitals increases smoothly, while that of the high K ones declines. This is connected with the nuclear shape evolution from an oblate to a prolate. As a result, one can conclude that the pairing effects can smear out all the abrupt changes in single-particle structure existing in the results without pairing, and thus for the neutrons, it leads to a smooth and gradual shape evolution from an oblate to a prolate. Because the proton density distributions often tend to have the largest overlap with the neutron ones so as to obtain the lowest energy, the proton density distributions evolve in a similar manner as the neutron ones with the increasing neutron number, and thus the quadrupole moments increase in an almost linear way with the increasing neutron number and cross zero in the middle.

This is not the full story, however. To investigate the importance of the core polarization effects, which are fully taken into account in the present work, one can extract the "corelike" quadrupole moments by excluding the contributions of valence nucleons, as shown in Fig. 3, from the total quadrupole moments. Since a full model space is taken in our calculations, we do not need to introduce the effective charges. Instead, the free charge is used in the present calculation, and thus the quadrupole moments are completely from the protons. Since $Z = 40$ is a typical subshell closure, it is straightforward to regard the 48 protons in Cd isotopes as a $Z = 40$ core coupled to 8 valence protons in the $g_{9/2}$ shell.
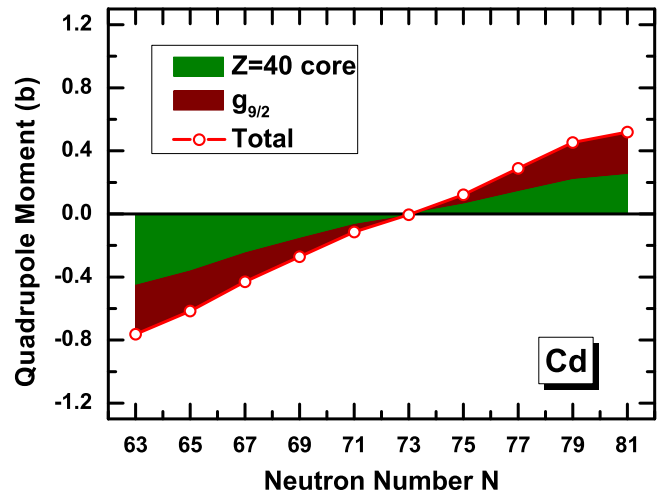

FIG. 3. (Color online) Composition of the total quadrupole moments as a function of the neutron number for the Cd isotopes. It is shown that the $Z = 40$ core contributes almost the same as the $g_{9/2}$ valence protons to the total quadrupole moments.

In Fig. 3, the compositions of the total quadrupole moments are shown as functions of the neutron number for the Cd isotopes. It is found that the core contributes almost the same as the valence protons to the total quadrupole moments. This core polarization also explains the relatively large effective charge $2.5e$ artificially introduced in Ref. [8]. Moreover, the quadrupole moments from both the core and the valence protons follow a linear increase behavior. This demonstrates that the core is strongly polarized and its coupling with the valence protons is very remarkable. Therefore, it is of importance to emphasize that polarization effects play a very important role in the self-consistent microscopic description of nuclear quadrupole moments.

Finally, it should be mentioned that apart from the $11/2^-$ quadrupole moments, the five $3/2^+$ quadrupole moments measured in Ref. [8] are also shown in the inset of the upper panel in Fig. 1 in comparison with the calculated results. One can see that the experimental data can be reproduced quite well, except for the notable deviation for $N = 73$ which may be due to the strong K mixing and needs to be investigated in further detail in the future. For the magnetic moments, however, it is a long-standing conundrum, which is essentially associated with the treatment of the coupling to complex configurations such as particle-vibration coupling (Arima-Horie effect [23,24]), meson exchange current, and core polarization effects [25–27].

In summary, for the first time, the simplicity in the nuclear quadrupole moments has been explained in a fully self-consistent and microscopic way with the covariant density functional theory. The newly observed quadrupole moments data for $^{107-129}$Cd together with their linear increase tendency with the neutron number are excellently reproduced without any *ad hoc* parameters. Instead of the linear neutron occupation mechanism in the $h_{11/2}$ shell, the simplicity of the linear increase is revealed to be due to the pairing correlation which smears out the abrupt changes induced by the single-particle shell structure, and thus leads to a smooth shape evolution.

Furthermore, it is found that the core is strongly coupled with the valence nucleons, and thus the core polarization effects turn out to be essential and contribute almost half of the total quadrupole moments.

[1] A. Bohr and B. R. Mottelson, *Nuclear Structure Volume I: Single-Particle Motion* (Benjamin, New York, 1969).

[2] J. M. B. Kellogg, I. I. Rabi, N. F. Ramsey, and J. R. Zacharias, Phys. Rev. **55**, 318 (1939).

[3] H. A. Bethe, Phys. Rev. **55**, 1261 (1939).

[4] T. Otsuka, T. Suzuki, R. Fujimoto, H. Grawe, and Y. Akaishi, Phys. Rev. Lett. **95**, 232502 (2005).

[5] R. A. Bark, J. F. Sharpey-Schafer, S. M. Maliage, T. E. Madiba, F. S. Komati, E. A. Lawrie, J. J. Lawrie, R. Lindsay, P. Maine, S. M. Mullins *et al*., Phys. Rev. Lett. **104**, 022501 (2010).

[6] K. Heyde and J. L. Wood, Rev. Mod. Phys. **83**, 1467 (2011).

[7] R. Chevrier, J. M. Daugas, L. Gaudefroy, Y. Ichikawa, H. Ueno, M. Hass, H. Haas, S. Cottenier, N. Aoi, K. Asahi *et al*., Phys. Rev. Lett. **108**, 162501 (2012).

[8] D. T. Yordanov, D. L. Balabanski, J. Bieroń, M. L. Bissell, K. Blaum, I. Budinčević, S. Fritzsche, N. Frömmgen, G. Georgiev, C. Geppert *et al*., Phys. Rev. Lett. **110**, 192501 (2013).

[9] G. Neyens, Rep. Prog. Phys. **66**, 633 (2003).

[10] J. L. Wood, Physics **6**, 52 (2013).

[11] M. G. Mayer and J. Jensen, *Elementary Theory of Nuclear Shell Structure* (Wiley, New York, 1955).

[12] H. Sagawa and A. Arima, Phys. Lett. B **202**, 15 (1988).

[13] H. Horie and A. Arima, Phys. Rev. **99**, 778 (1955).

[14] A. de Shalit and I. Talmi, *Nuclear Shell Theory* (Academic, New York, 1963).

[15] P. Ring, Prog. Part. Nucl. Phys. **37**, 193 (1996).

[16] D. Vretenar, A. V. Afanasjev, G. A. Lalazissis, and P. Ring, Phys. Rep. **409**, 101 (2005).

[17] J. Meng, H. Toki, S. Zhou, S. Zhang, W. Long, and L. Geng, Prog. Part. Nucl. Phys. **57**, 470 (2006).

[18] J. Meng, J. Peng, S.-Q. Zhang, and P.-W. Zhao, Frontiers Phys. **8**, 55 (2013).

[19] P. Ring, Phys. Scr. T **150**, 014035 (2012).

[20] P. Ring, Y. K. Gambhir, and G. A. Lalazissis, Comput. Phys. Commun. **105**, 77 (1997).

[21] P. W. Zhao, Z. P. Li, J. M. Yao, and J. Meng, Phys. Rev. C **82**, 054319 (2010).

[22] P. Ring and P. Schuck, *The Nuclear Many-Body Problem* (Springer-Verlag, New York, 1980).

[23] A. Arima and H. Horie, Prog. Theor. Phys. **11**, 509 (1954).

[24] A. Arima, Sci. China Phys. Mech. Astron. **54**, 188 (2011).

[25] I. S. Towner, Phys. Rep. **155**, 263 (1987).

[26] A. Arima, K. Shimizu, W. Bentz, and H. Hyuga, Adv. Nucl. Phys. **18**, 1 (1987).

[27] J. Li, J. Meng, P. Ring, J. M. Yao, and A. Arima, Sci. China Phys. Mech. Astron. **54**, 204 (2011).